ELSEVIER

Thermochimica Acta 282/283 (1996) 91–100

thermochimica acta

The complex DSC analysis of the first crystallization peak of Fe_{80} Si_{10} B_{10} metallic glass[1]

Emília Illeková [a,*], Federica Malizia [b], F. Ronconi [b]

[a] *Institute of Physics, Slovak Academy of Sciences, Dúbravská cesta 9, 842 28 Bratislava, Slovak Republic*

[a] *Dipartimento di Fisica, Universita di Ferrara, Via Paradiso 12, 44100 Ferrara, Italy*

Abstract

The crystallization of Fe_{80} Si_{10} B_{10} glass was studied both by linear heating and isothermal differential scanning calorimetry (DSC). Two well separated crystallization peaks were always observed. On the basis of the classical isothermal Johnson–Mehl–Avrami (JMA) procedure both transient nucleation and transient growth kinetics with the complex exponent $n \sim 2.8$ and mean activation energy $E^*_{JMA} = 323$ kJ mol^{-1} were determined for the first crystallization peak. Because for the degree of conversion $\alpha > 0.55$ $E^*(\alpha)$ dependence was observed, the deconvolution of the isothermal peak into the subsequent JMA nucleation-and-growth and grain-growth effects was used to fit the measured data. Simple JMA kinetics could not be determined for the linear heating first crystallization peak. All these results correlate with structural analysis studies.

Keywords: Crystallization kinetics; DSC; Fe_{80} Si_{10} B_{10} glass; Johnson–Mehl–Avrami model

1. Introduction

Metallic glasses are, because of their extremely rapid solidification technology, solids with a high degree of non-equilibrium. Generally, they are heterogeneous and often also anisotropic. At elevated temperatures, usually before reaching the undercooled liquid state or subsequent to the glass transition, they spontaneously transform to the crystalline or partially crystalline states. In the second case no exact proof of long-range diffusion-controlled primary crystallization, eutectic deconvolution or polymorphous

* Corresponding author.

[1] Dedicated to Takeo Ozawa on the Occasion of his 65th Birthday.

PII S0040-6031(96)02881-X

transformation in the already existing supersaturated solid solution regions has yet been given.

The crystallization of metallic glasses is characterized by a sharp, often asymmetric, differential scanning calorimetry (DSC) peak having transformation enthalpy ΔH_{tot} of the order of 100 J g^{-1}. Because of the complicated character of the transformation being discussed, none of the existing model solid-state kinetic equations is suitable to describe it. Nevertheless, Johnson–Mehl–Avrami (JMA) kinetics are assumed to be generally valid [1] and in some cases fit the experimental data quite well [2].

In this paper the kinetics of the first DSC crystallization peak of Fe_{80} Si_{10} B_{10} metallic glass is studied both by linear heating and isothermal measuring regimes. The Kissinger [3], ($\ln(w^+/T_p^2)$ vs $1/T_p$), and isoconversional [4], ($\ln(dH/dt)_\alpha$ vs $1/T_a$) and ($\ln(dH/dT)_\alpha$ vs $1/T_\alpha$),methods as well as JMA fitting procedures [5,4], ($\ln(-\ln(1-\alpha))$ vs $\ln t_\alpha$) and $(dH/dt = \Delta H_{tot} n(1-\alpha)[-\ln(1-\alpha)]^{(n-1)/n} A \exp(-E^*_{JMA}/RT))$, are used, where w^+ is the heating rate, T_p is the linear heating peak temperature, dH/dt or dH/dT are the measured isothermal or linear heating DSC signals, α is the degree of conversion, T_a is the isothermal annealing temperature, and n, A and E^*_{JMA} are the JMA exponent, pre-exponential factor and activation energy. By such a complex analysis of the kinetics the assumed JMA mechanism of crystallization of the glassy samples will be tested and the alternative deconvolution of both isothermal and continuous heating peaks will be studied.

2. Experimental

The 21 μm thick Fe_{80} Si_{10} B_{10} metalic ribbons were prepared by the planar flow casting technique (the quenching rate $w^- \sim -10^{-7}$ K s^{-1}). Their amorphous nature was tested by X-ray diffraction and electron microscopy. The measurements of as-quenched samples were performed with a Perkin–Elmer DSC7 instrument using the linear heating technique with w^+ from 5 to 80 K min^{-1} and the isothermal technique having the heating ramp with $w^+ = 40$ K min^{-1}. In both cases the subtraction of two successive measurements under the same conditions was used for calculations. Five milligram samples, the empty pan reference and argon atmosphere were used.

The temperature and enthalpy axes of the DSC instrument were callibrated by the use of indium and zinc standards for all heating rates. Afterwards no heating rate influence on the Curie point of nickel was observed.

3. Results and discussion

The crystallization of Fe_{80} Si_{10} B_{10} glass always consists of two well separated exothermal peaks. The influence of the heating rate, w^+, on the linear heating DSC thermograms is seen in Fig. 1. The dependence of the first isothermal crystallization peak on annealing temperature, T_a, is seen in Fig. 2. The temperature interval where the isothermal crystallization effect could be seen in experimental real time was limited to 30 K, namely, in the temperature range 733–763 K, the temperatures which precede the

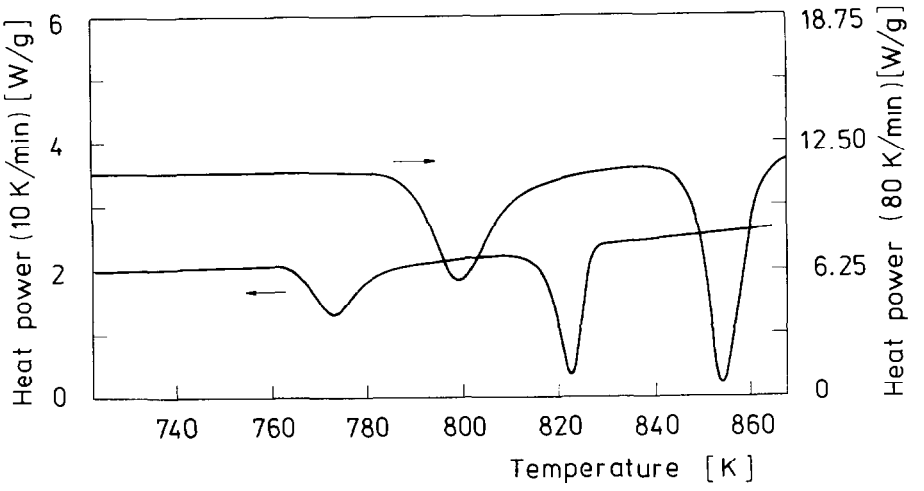

Fig. 1. The linear heating DSC traces of crystallization of $Fe_{80}Si_{10}B_{10}$ glass at heating rates of 10 and 80 K min^{-1}.

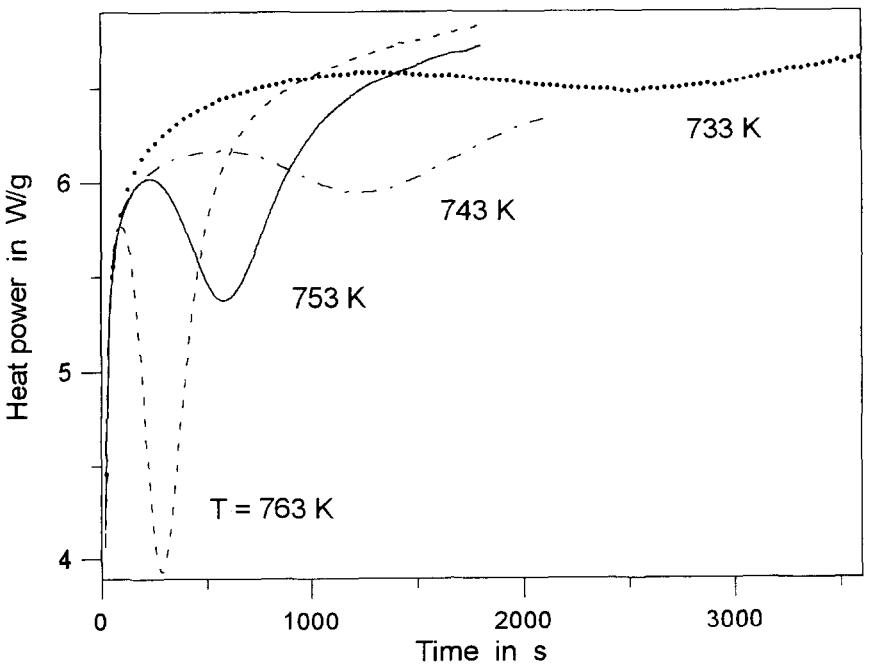

Fig. 2. The isothermal DSC traces of crystallization of $Fe_{80}Si_{10}B_{10}$ glass (the temperature T_a being a parameter).

onset temperature of the linear heating crystallization $T_x = 763$ K of the material($w^+ = 10$ K min^{-1}).

Because the difference between the glass-like and crystal-like specific heats of $Fe_{80}Si_{10}B_{10}$ is very small in relation to the height of the crystallization apparent specific heat peak, the straight line between the first and last peak points could be used as the baseline for $\Delta H_{tot} = \int_{\alpha=0}^{\alpha=1}(dH/dt)dt$ or $\Delta H_{tot} = \int_{\alpha=0}^{\alpha=1}(dH/dT)dT$ and $\alpha = \Delta H(\alpha)/\Delta H_{tot}$ calculations.

If the kinetics of the crystallization are JMA-like

$$\alpha = 1 - \exp[-(kt)^n] \tag{1}$$

and the rate constant k is the Arrhenius-like

$$k = A\exp[-E^*_{JMA}/RT)] \tag{2}$$

where A, E^*_{JMA} and n are the JMA constants and R is the gas constant, then in the isothermal case

$$\ln[-\ln(1-\alpha)] = n\ln[k(T_a)] + n\ln t_\alpha \tag{3}$$

If the assumed linearity was not observed then some time lag, τ, can be found for each isotherm and subtracted from the real experimental time, t_α, to linearize Eq. (3), following the Thompson, Greer, and Spaepen procedure [5]. This mathematical formalism is equivalent to the assumption of the existence of transient nucleation rate in the JMA kinetics.

The classical JMA representations, Eq. (3), of the isothermal exotherms from Fig. 2 were always non-linear, as is shown by the curve constructed using the full symbols in Fig. 3. The effective time lags, τ, which were always considerably higher than the experimental incubation times, τ_{exp}, starting the isothermal crystallization peaks, were

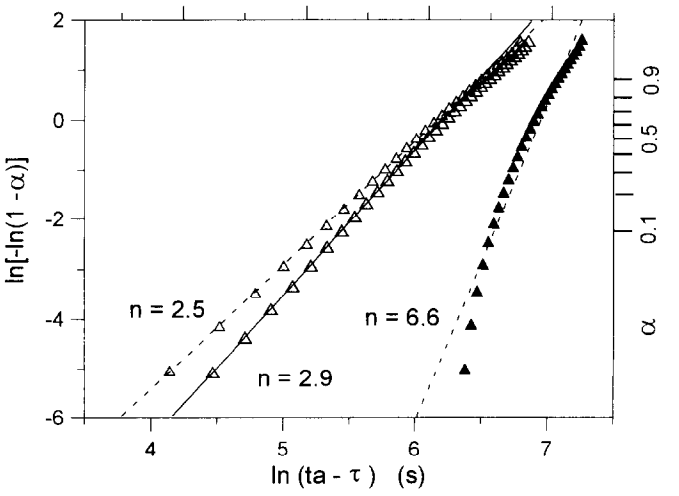

Fig. 3. The calculated JMA plots (Eq. (3)), (▲) and by subtracting the time lags, $\tau = 471$ s and 495 s, from the experimental real time, t, straightened JMA plots, (△) and (△), for $\alpha \in (0, 0.55 >$ (\rangle in LATEX) and (0, 1), respectively, for the isothermal first crystallization peak of $Fe_{80}Si_{10}B_{10}$ glass at $T_a = 753$ K from Fig. 2. Avrami exponents, n, being the parameters, are the slopes of the linear fits (dashed and full lines).

Table 1
Parameters estimated from Eq. (3) for the first crystallization stage of $Fe_{80}Si_{10}B_{10}$ for each isothermal annealing temperature T_a and $\alpha \in (0, 0.5 > (\backslash rangle$ in LATEX) τ_{exp} is the experimental incubation time; τ, k and n the time lag, the rate constant and the Avrami exponent, are the linearization fitting parameters; $n^{\#}$ is the linearization fitting parameter if $\tau = 0$ and $\alpha \in (0, 1)$

T_a/K	τ_{exp}/s	τ/s	$\ln k/s^{-1}$	n	$n^{\#}$
733	1221	1399	−7.59	2.64	5.54
743	430	705	−6.87	3.12	6.48
753	212	471	−6.20	2.92	6.59
753	257	516	−6.17	2.66	6.40
763	95	370	−5.50	2.84	6.90

found and the dependences, Eq. (3), were linearized as shown by the curves constructed using the empty symbols in Fig. 3). The set of final fitting parameters, τ_{exp}, τ, n and k, is provided in Table 1 for all considered temperatures. It was also found that because of this linearization the unrealistically high values of $n(>6)$, being the slopes of the dependences, Eq. (3), were modified to be $n \sim 2.7$, if $\alpha \in (0, 1)$, or $n \sim 2.8$, only if $\alpha \in (0, 0.55 > (\backslash rangle$ in LATEX)(the dashed and full lines in Fig. 3). These exponents indicate the zero nucleation rate and the decreasing growth rate, the extent of which depends on α being taken into account. Besides, knowing the temperature-dependence of the rate constant $k(T_a)$, which is given by Eq. (2), $E^*_{JMA} = (323 \pm 3)$ kJ mol^{-1} and $\ln A = (45.4 \pm 0.5)$ were calculated (A being in s^{-1}) in both cases.

In the case of well defined kinetics the T and α dependences can be separated into

$$d\alpha/dt = k(T) f(\alpha) \tag{4}$$

and in the moments (T_α, t_α) having a constant degree of conversion α

$$\ln(d\alpha/dt)_\alpha = \text{const} - E^*/(RT_\alpha) \tag{5}$$

Then using the isothermal isoconversional method, the slope of the measured isothermal DSC signals at various T_a, $\ln(dH/dt)_\alpha$ vs $1/T_a$ gives the activation energy E^*_I or, using the linear heating isoconversional method in the case of several dynamic DSC curves measured at various w^+, the slope of $\ln(dH/dT)_\alpha$ vs $1/T_\alpha$ gives the activation energy, E^*_{CH}. Fig. 4 shows the correlation between both calculated quantities, being $E^*_I = (382 \pm 15)$ kJ mol^{-1} and $E^*_{CH} = (368 \pm 11)$ kJ mol^{-1} for $\alpha = 0.1$. The systematic shift between the isothermal and linear heating lines in Fig. 4 reflects the complexity of the kinetic equation, Eq. (1). Several authors (e.g. Šesták et al. [6]) have shown the difference between the expressions for the isothermal and non-isothermal rate constants. The calculated correction [7] may lead to such differences as were observed in our case.

On the basis of isoconversional methods the constancy of the activation energy of transformation can be proved. In our isothermal crystallization events this was true for

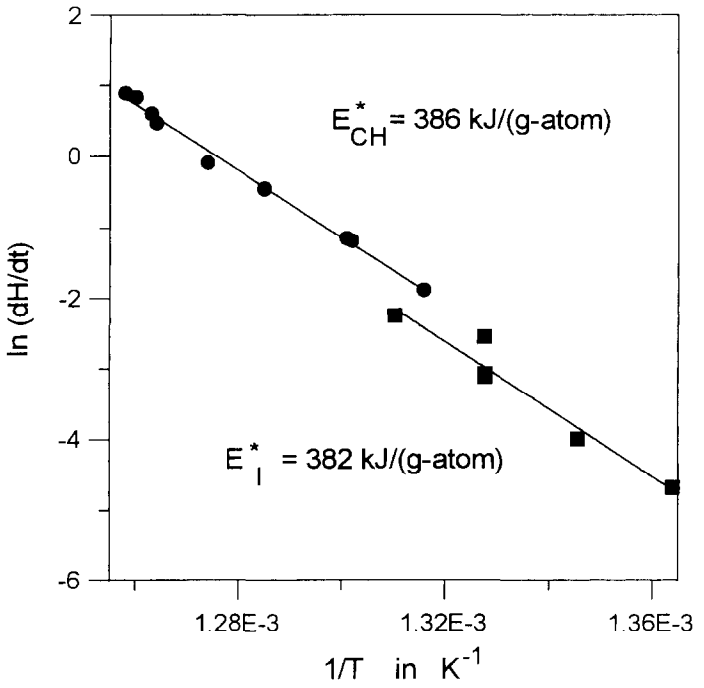

Fig. 4. Isoconversional method plots of $(dH/dt)_\alpha$ in logarithmic form versus $1/T_\alpha$ for a fixed degree of conversion $\alpha = 0.1$: (■) isothermal data; (●) linear heating data of the first crystallization peak of $Fe_{80}Si_{10}B_{10}$ glass, (activation energies being the parameters are proportional to the slopes of —— lines).

$\alpha < 0.55$. In the case of $\alpha > 0.55$ some other process probably had to contribute (see Fig. 5). In the linear heating regime the situation was much more complicated (see Fig. 6).

It was not possible to interpret the linear heating crystallization peaks by any single JMA kinetics for the whole $\alpha \in (0, 1)$ interval, probably beacuse of the presence of several processes. Nevertheless the Kissinger activation energy, being $E_K^* = (381 \pm 10)$ kJ mol^{-1} correlates well with both quantities E_I^* and E_{CH}^*. This finding means that independently of the heating rate, w^+, the same rate controlling process always prevails in the moments of the dynamic DSC peak ($\alpha_{min} = 0.63$).

On the basis of the previous thermal analysis results [8, 9] and of the electron microscopy [9] and Mossbauer [10, 11] observation of the crystallization of Fe–B and Fe–Si–B glasses the superimposition of independent JMA nucleation-and-growth crystallization (Eq. (1) and subsequent coarsening of the crystallizing grains by the grain-growth mechanism [12, 13] can also be assumed here:

$$dH/dt = (dH/dt)_{NG} + (dH/dt)_{GG} \tag{6}$$

$$(dH/dt)_{NG} = \Delta H_{tot} n k^n (t - \tau)^{n-1} \exp\{-[k(t - \tau)]^n\} \tag{7}$$

$$(dH/dt)_{GG} = (H_0 r_0/m)(K/[r_0^m + K(t - \tau_s)]^{(m+1)/m}) \tag{8}$$

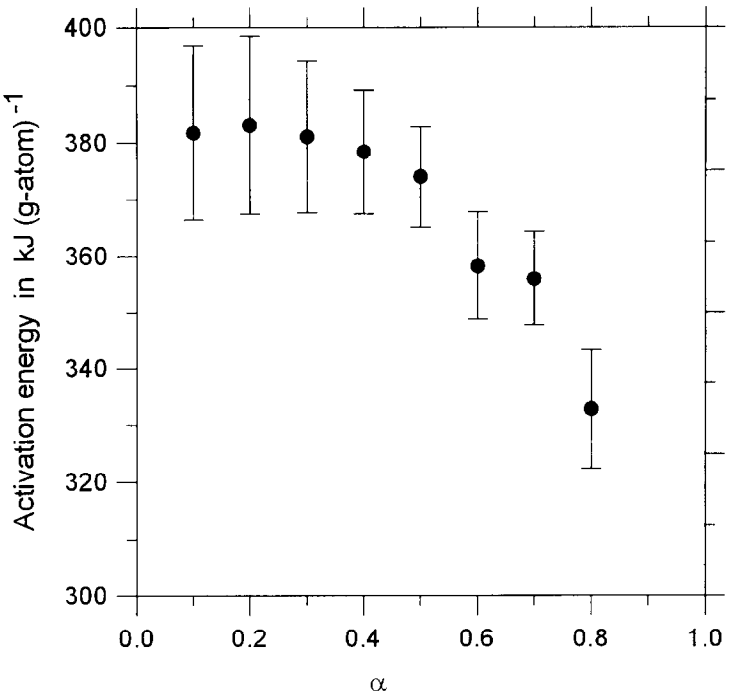

Fig. 5. The dependence of the isoconversional-method-calculated activation energy of the first isothermal crystallization peak of $Fe_{80}Si_{10}B_{10}$ glass on the degree of conversion α.

where H_0 and r_0 are the initial enthalpy and the grain radius, respectively, τ_s is the time at which the coarsening starts to work, m is the grain-growth exponent, $K(T) = mcM(T)\lambda^m\gamma$ is the Arrhenius-like grain-growth rate constant, and Z is a constant. In Fig. 7 the deconvolution of the isothermal crystallization peak at $T_a = 753$ K is shown. The kinetic exponents and incubation times starting the processes considered, namely, $n = 3.0$, $\tau = 151.5$ s for the JMA nucleation-and-growth process and $m = 2.4$, $\tau_s = 729.8$ s for the grain-growth process were deduced. The details concerning our model and the procedure for optimization of parameters are described in Refs. [8 and 9].

4. Conclusions

The contemporary models of structural relaxation and crystallization in metallic Fe–Si–B glasses are based on short-range ordered clusters surrounded by an amorphous matrix with a structure not yet described. The relationship between the ordering inside the clusters in the amorphous matrix, and the future crystals is not yet known. The crystallization of such a complicated non-equilibrium solid structure at tempera-

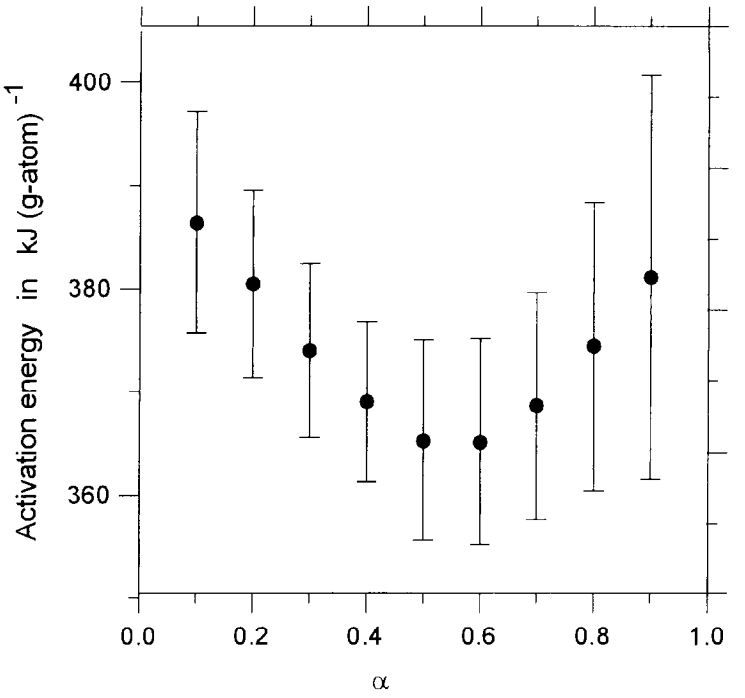

Fig. 6. The dependence of the isoconversional-method-calculated activation energy of the first linear heating crystallization peak of $Fe_{80}Si_{10}B_{10}$ glass on the degree of conversion α.

tures much lower than that of equilibrium crystallization is seen to be a complicated multi-process in time and temperature. Both isothermally and in the linear heating regime several processes cooperate.

On the basis of complex DSC kinetic analysis, the first crystalline phase in the glassy $Fe_{80}Si_{10}B_{10}$ ribbon is formed by JMA nucleation-and-growth process (n = 2.8). After some time lag, τ_s, (being 730 s at 753 K) these microcrystals start to coarsen by the grain-growth mechanism (m = 2.4), and this process is finished after a relatively long time (or at substantially higher temperatures) by the next stage of crystallization.

For $\alpha < 0.55$, the mean value of the apparent activation energy of the isothermal first crystallization peak $E_I^* \sim 381$ kJ mol^{-1} characterizes the first nucleation-and-growth process, $E_I^*(\alpha) = E_{NG}^*$. After the time lag $\tau_s(T_a)$, this means that for $\alpha > 0.55$, $E_I^*(\alpha)$ continually changes its absolute value into that for grain growth ($E_{GG}^* \ll E_{NG}^*$). (This quantity was studied by the isothermal isoconfigurational method.) Fitting the crystallization DSC peak using the previously standard assumption of only one classical JMA nucleation-and-growth kinetic equation (Eq. (3)) shows the importance or transient nucleation and growth phenomena, the exponent $\bar{n} = 2.8$, however $E_{JMA}^* = 323$ kJ mol^{-1} is the mean value of our model hypothetical values of E_{NG}^* and E_{GG}^*.

Because $\tau_s(T)$ is Arrhenius-like temperature-dependent (Table 1), the overlapping of the participating nucleation-and-growth and grain-growth processes is also tempera-

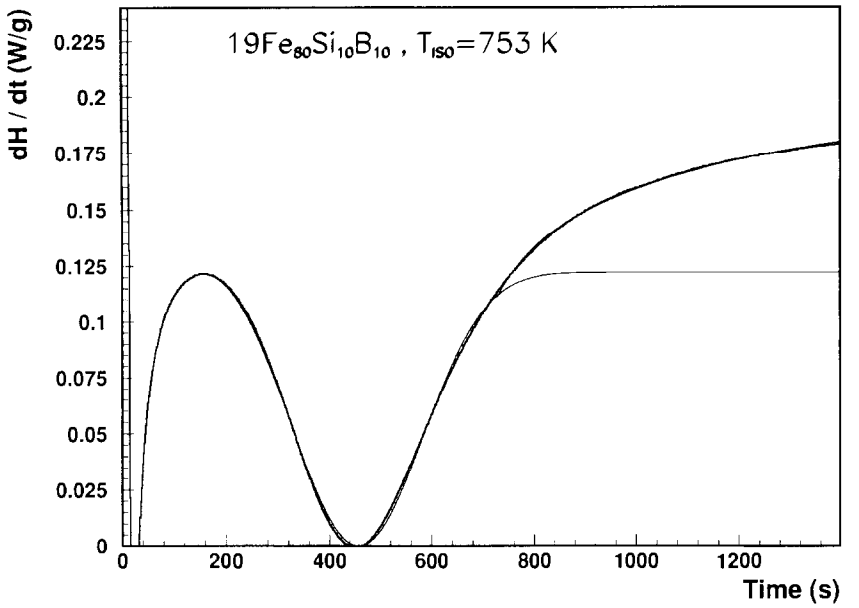

Fig. 7. The deconvolution of the first isothermal crystallization peak of $Fe_{80}Si_{10}B_{10}$ glass measured at $T_a = 753$ K, (——), to the JMA nucleation-and-growth process, (——), with $n = 2.985$, $\ln k = -5.09$ (k in s^{-1}), $\tau = 151.52$ s, $\Delta H_{tot} = 36.639$ J g^{-1} s and grain-growth process with $m = 2.41$, $cM\gamma = 0.961$ s^{-1}, $\lambda = 0.305$ μm, $\tau_s = 729.77$ s, $r_0 = 0.88$ μm, $H_0 = 115.73$ J g^{-1}.

ture-dependent in the dynamic measurements. Therefore $E^*_{CH}(\alpha)$, calculated by the linear heating isoconversional method, is not constant and its absolute value has no physical meaning. The superimposition of more processes is evident in this case. The calculated mean Kissinger activation energy, E^*_K, (which quantitatively agrees with E^*_I and E^*_{NG} refers to that of the main continuous heating process.

X-ray diffraction and electron microscopy studies of the crystallization of $Fe_{80}Si_{10}B_{10}$ glassy ribbons support this model [14].

References

[1] A.L. Greer, in S. Steeb and H. Warlimont (Eds.), Rapidly Quenched Materials, Elsevier Science, Amsterdam, 1985, p. 215.
[2] A.L. Greer, Acta Metall., 30 (1982) 171.
[3] H.E. Kissinger, Anal. Chem., 29 (1957) 1702.
[4] TA-system, Software for thermal analysis, (TriloByte, Ltd, Praha 1991).
[5] C.V. Thompson, A.L. Greer and F. Spaepen, Acta Metall, 31 (1983) 1883.
[6] J. Šesták, V. Šatava and W.W. Wendlandt, Thermochim. Acta, 7 (1973) 447.
[7] E. Urbanovič and S. Segal, ICTA Bulletin, Review article No3 (1995) 13.
[8] F. Malizia and F. Roconi, Philos. Mag., B68 (1993) 869.

[9] F. Malizia and F. Roconi, J. Appl. Phys., 74 (1993) 6988.
[10] F. Malizia and F. Roconi, Proc. of Am. Mater. Res. Soc., Fall Meeting, 1994 (Boston 1994
[11] F. Malizia and F. Ronconi, J. Magn. Magn. Mater., 133 (1994) 295.
[12] H.V. Atkinson, Acta Metall., 36 (1988) 469.
[13] L.C. Chen and F. Spaepen, J. Appl. Phys., 69 (1991) 679.
[14] I. Maťko, E. Illeková, P. Duhaj and P. Švec, Mater. Sci. Eng., in preparation.